Supplementary Results : Genome admixture components are not significant predictors of phenotypes that depend on tight genotype × genotype interactions.

Polygenic adaptation is not expected for phenotypes measuring association with symbiotic bacteria because of the tight genotype × genotype interactions which govern these plant-symbiont interactions[71]. However signatures of selection have been reported for only a few genes involved in the control of symbiotic nitrogen fixation[47;66]. We thus test the WhoGEMM approach by looking for relationships between admixture component proportions and quantitative phenotypes measuring association to symbiotic nitrogen fixation bacteria.

Supplementary Figures 11a, 11b and 11c depict the geographical structure of nodule numbers in different root parts, used as a proxies to test for nodulation efficiency[64]. The spatial patterns for each nodulation phenotype are complex and little correspondence appears between nodulation in upper and lower root parts. Ancestral genome proportions are significantly related to nodulation efficiency in the top 5cm of the roots (Supplementary Table 6d ; r^2 =0.15, P =1.1×10^{-8}), but only to a much lower extent in the region below 5cm (Supplementary Table 6c ; r^2 =0.06, P =4.2×10^{-4}). Consequently, the total number of nodules per root is only moderately related to admixture proportions (Supplementary Table 6e; r^2 =0.1, P =5.999×10^{-6}) in that experiment.

The analysis reported by Stanton-Geddes *et al.*[64] used a mix of two different strains of *S. meliloti* simultaneously applied to all accessions in a common-garden design. In that experiment, the number of nodules (whether using the total, upper or lower 5cm of root) was not correlated to plant height or number of leaves (Supplementary Table 10), indicating that symbiosis was not efficiently engaged between the host plants and the selected microbial symbiotic strains. This unexpected fact, not discussed by the authors, may preclude any further conclusions on symbiosis efficiency and putative adaptation to given symbionts in this particular experimental design. It is also reported that some *M. truncatula* accessions present better performances with *S. medicae* strains rather than *S. meliloti* strains. The procedure described by Stanton-Geddes *et al.*[64] thus probably masks putative local adaptations to particular symbiont strains.

The weak relationship between nodulation performances and population structure contrasts with the situation for plant height, or quantitative resistances towards *V. alfalfae* or *A. euteiches*. This finding suggests that adaptation to local strains of rhizobia plays an important role, re-inforcing the genotype × genotype interaction hypothesis for the control of symbiotic nitrogen fixation.

Supplementary Tables legends

Supplementary Table 1: SNP selection process for admixture analysis.
Quality Checked (QC) SNPs : genotyping rate ≥ 0.95 and Minor Allele Frequency ≥ 0.01. LD-pruned SNPs : Variance Inflation Factor ≤ 1.22 in a window of 300 SNPs.

Supplementary Table 2: Classification of 262 *Medicago truncatula* accessions in 8 populations, based on their admixture components defined by supervised amixture analysis.

Supplementary Table 3: Correlations between admixture components and 19 bioclimatic variables defined by WorldClim.

Supplementary Table 4: p-values for significances of correlations between admixture components and 19 bioclimatic variables defined by WorldClim.
FDR=0.05.

Supplementary Table 5: Linear model between admixture components and root rot index due to infection of *M. truncatula* by *Aphanomyces euteiches*.
Data from Bonhomme *et al.*[45]

Supplementary Table 6: Linear models between *M. truncatula* admixture components and several quantitative functional traits.
(a) Linear model between admixture components and number of nodules below 5 cm of root growth. (b) Linear model between admixture components and number of nodules in top 5 cm of roots. (c) Linear model between admixture components and total number of nodules. (d) Linear model between admixture components and plant height (final height before harvest). (e) Linear model between admixture components and number of leaves at about two weeks. For each phenotype, the scale from low values (blue) to high values (red) is indicated on the right. Raw data from Stanton-Geddes *et al.*[64]

Supplementary Table 7: Annotation of genes with significant purifying selection in the eight *M. truncatula* populations.
Genome Mt4.0 and annotation Mt4.0v2 were used for computations.

Supplementary Table 8: Genes putatively under positive selection in at least one *M. truncatula* population, as determined by dN/dS analysis.
Genome Mt4.0 and annotation Mt4.0v2 were used for computations.

Supplementary Table 9: Annotation of genes with putative positive selection differing among the eight *M. truncatula* populations.
Genome Mt4.0 and annotation Mt4.0v2 were used for computations.

Supplementary Table 10: Correlations between symbiosis-related traits.
Data from Stanton-Geddes *et al.*[64]

Supplementary Table 11: Maximum symptom score of 262 *M. truncatula* accessions in response to root infection by *Verticillium alfalfae*.
See Supplementary Table 2 for population classification.

Supplementary Table 12: Maximum symptom score of 71 previously uncharacterized *M. truncatula* accessions in response to root infection by *Verticillium alfalfae*.
Expected phenotype, based on their geographical closeness with resistant or susceptible reference accessions (see Supplementary Table 11) is reported.

Supplementary Figures legends

Supplementary Figure 1: Splitting patterns of accessions' sets, based on clustering by admixture components, as K increases from $K = 3$ to $K = 11$.
Dashed line indicates minor contribution of a population. Accessions's sets are labelled following their major genome component.

Supplementary Figure 2: PCA plot of 262 *M. truncatula* accessions and the $K = 7$ putative ancestral populations, for pairwise comparisons of the first six eigenvectors.
Coloured points represent simulated individuals, one colour per admixture component.

Supplementary Figure 3: PCA plot of 262 *M. truncatula* accessions and the $K = 8$ putative ancestral populations, for pairwise comparisons of the first six eigenvectors.
Coloured points represent simulated individuals, one colour per admixture component.

Supplementary Figure 4: PCA plot of 262 *M. truncatula* accessions and the $K = 9$ putative ancestral populations, for pairwise comparisons of the first six eigenvectors.
Coloured points represent simulated individuals, one colour per admixture component.

Supplementary Figure 5: PCA plot of 262 *M. truncatula* accessions and the $K = 10$ putative ancestral populations, for pairwise comparisons of the first six eigenvectors.
Coloured points represent simulated individuals, one colour per admixture component.

Supplementary Figure 6: Predicted distance from true origin for each *M. truncatula* accession using the leave-one-out procedure, for increasing values of K.
Empirical curve for K = 8 is displayed in bold.

Supplementary Figure 7: Hierarchical clustering of 262 *M. truncatula* accessions based on their admixture proportions, after supervised admixture analysis with $K = 8$ putative ancestral genomes.
Each color corresponds to a given component. Color coding is the same as Figure 2

Supplementary Figure 8: Dendrogam of genetic relationships between representative accessions of the eight *M. truncatula* populations, based on analysis of the 840K SNP dataset.
Color coding is the same as Figure 2

Supplementary Figure 9: *M. truncatula* accessions repartition within Mediterranean Basin climatic zones following Köppen-Geiger climate classification.

Supplementary Figure 10: Geographical repartition of root-rot index following infection of 174 *M. truncatula* accessions by *Aphanomyces euteiches*.
At each evaluated accession, a pie chart present the admixture patterns of it. Scale of index from resistant (blue) to susceptible (red) accessions is indicated on the right. Raw data from Bonhomme *et al.*[45].

Supplementary Figure 11: Geographical repartition of phenotypes for several quantitative functional traits in 226 *M. truncatula* accessions.
(a) number of nodules below 5 cm of root growth. (b) number of nodules in top 5 cm of roots. (c) total number of nodules. (d) final plant height before harvest (e) number of leaves at about two weeks. Data from Stanton-Geddes *et al.*[64]

Supplementary Figure 12: Relation between geographical and genetic distances among 245 *M. truncatula* accessions with known location, for $K = 8$.
The red dotted curve is a loess adjusted curve. The vertical blue line is drawn at 950km.

Supplementary Figure 13: Predicted distance from true origin for *M. truncatula* accessions using the 'leave-one-out' procedure for Geographic Population Structure based genome admixture proportions determined by supervised admixture analysis.

chromosome	Avail. SNPs	QC SNPs	LD-pruned SNPs
Chrom. 1	4 978 489	158 858	116 038
Chrom. 2	4 331 584	136 735	100 011
Chrom. 3	5 424 868	165 394	121 174
Chrom. 4	5 414 544	170 726	123 580
Chrom. 5	4 496 375	133 727	98 578
Chrom. 6	3 650 081	97 328	72 271
Chrom. 7	4 761 519	151 101	111 584
Chrom. 8	4 377 934	135 847	99 935
total	37 435 394	1 149 716	843 171

Supplementary Table 1

Bioclimatic variable	Type	Algiers	Spanish Coastal	North Tunisian Coastal	Atlas	South Tunisian Coastal	French	Greek	Spanish-Morocco Inland
BIO1: Annual Mean Temperature	Annual trend	-0.13	0.03	0.16	-0.05	0.26	-0.45	0.12	0.08
BIO2: Mean Diurnal Range (Mean of monthly (max temp - min temp))	Seasonality	-0.15	-0.16	0.1	0.4	0.02	-0.48	-0.09	0.18
BIO3: Isothermality (BIO2/BIO7) (* 100)	Seasonality	-0.26	0.15	0.09	0.08	0.15	-0.42	-0.02	0.18
BIO4: Temperature Seasonality (standard deviation *100)	Seasonality	0.1	-0.42	0.05	0.47	-0.07	-0.25	-0.01	-0.06
BIO5: Max Temperature of Warmest Month	Extreme conditions	-0.09	-0.22	0.16	0.41	0.07	-0.6	-0.05	0.15
BIO6: Min Temperature of Coldest Month	Extreme conditions	-0.1	0.22	0.08	-0.29	0.2	-0.11	0.12	0.01
BIO7: Temperature Annual Range (BIO5-BIO6)	Seasonality	-0.01	-0.31	0.07	0.5	-0.07	-0.4	-0.11	0.11
BIO8: Mean Temperature of Wettest Quarter	Extreme conditions	-0.19	0.21	-0.02	-0.29	0.2	0.16	0.03	0.02
BIO9: Mean Temperature of Driest Quarter	Extreme conditions	-0.01	-0.17	0.13	0.17	0.14	-0.48	0.1	0.05
BIO10: Mean Temperature of Warmest Quarter	Extreme conditions	-0.06	-0.17	0.18	0.19	0.21	-0.57	0.07	0.08
BIO11: Mean Temperature of Coldest Quarter	Extreme conditions	-0.13	0.18	0.11	-0.21	0.24	-0.28	0.09	0.1
BIO12: Annual Precipitation	Annual trend	0.06	-0.01	-0.17	-0.03	-0.28	0.41	0.05	-0.08
BIO13: Precipitation of Wettest Month	Extreme conditions	0.05	-0.01	-0.16	-0.19	-0.12	0.1	0.39	-0.11
BIO14: Precipitation of Driest Month	Extreme conditions	-0.09	-0.07	-0.08	0	-0.1	0.56	-0.06	-0.17
BIO15: Precipitation Seasonality (Coefficient of Variation)	Seasonality	-0.01	0.08	-0.04	-0.3	0.15	-0.41	0.45	0.1
BIO16: Precipitation of Wettest Quarter	Extreme conditions	0.07	0.02	-0.17	-0.16	-0.16	0.12	0.33	-0.1
BIO17: Precipitation of Driest Quarter	Extreme conditions	-0.05	-0.08	-0.08	0.06	-0.13	0.62	-0.15	-0.2
BIO18: Precipitation of Warmest Quarter	Extreme conditions	-0.06	-0.08	-0.02	0.04	-0.08	0.65	-0.17	-0.25
BIO19: Precipitation of Coldest Quarter	Extreme conditions	0.08	0	-0.13	-0.09	-0.13	-0.03	0.29	-0.06

Supplementary Table 3

Bioclimatic variable	Algiers	Spanish Coastal	North Tunisian Coastal	Atlas	South Tunisian Coastal	French	Greek	Spanish-Morocco Inland
BIO1	1.000	1.000	1.000	1.000	0.004	0.000	1.000	1.000
BIO2	1.000	1.000	1.000	0.000	1.000	0.000	1.000	0.584
BIO3	0.005	1.000	1.000	1.000	1.000	0.000	1.000	0.445
BIO4	1.000	0.000	1.000	0.000	1.000	0.013	1.000	1.000
BIO5	1.000	0.063	1.000	0.000	1.000	0.000	1.000	1.000
BIO6	1.000	0.075	1.000	0.000	0.193	1.000	1.000	1.000
BIO7	1.000	0.000	1.000	0.000	1.000	0.000	1.000	1.000
BIO8	0.285	0.113	1.000	0.001	0.238	1.000	1.000	1.000
BIO9	1.000	0.655	1.000	0.827	1.000	0.000	1.000	1.000
BIO10	1.000	0.797	0.474	0.313	0.090	0.000	1.000	1.000
BIO11	1.000	0.453	1.000	0.094	0.025	0.001	1.000	1.000
BIO12	1.000	1.000	0.756	1.000	0.001	0.000	1.000	1.000
BIO13	1.000	1.000	1.000	0.278	1.000	1.000	0.000	1.000
BIO14	1.000	1.000	1.000	1.000	1.000	0.000	1.000	0.797
BIO15	1.000	1.000	1.000	0.000	1.000	0.000	0.000	1.000
BIO16	1.000	1.000	0.876	1.000	1.000	1.000	0.000	1.000
BIO17	1.000	1.000	1.000	1.000	1.000	0.000	1.000	0.175
BIO18	1.000	1.000	1.000	1.000	1.000	0.000	0.910	0.011
BIO19	1.000	1.000	1.000	1.000	1.000	1.000	0.000	1.000

Supplementary Table 4

	Estimate	Std. Error	t value	Pr(>|t|)
Intercept	2.7362	0.1237	22.12	0.0000
Algiers	-1.2335	0.2816	-4.38	0.0000
Spanish Coastal	-1.1635	0.2353	-4.95	0.0000
North Tunisian Coastal	-1.4798	0.3648	-4.06	0.0001
Atlas	-0.7511	0.1918	-3.92	0.0001
French	-0.5753	0.1963	-2.93	0.0038
Greek	-0.3084	0.1812	-1.70	0.0906

Supplementary Table 5

	Estimate	Std. Error	t value	Pr(>|t|)
intercept	14.1608	0.3506	40.39	0.0000
South Tunisian Coastal	5.7582	1.1345	5.08	0.0000
Greek	3.6659	0.6954	5.27	0.0000
North Tunisian Coastal	5.0274	1.1228	4.48	0.0000
Spanish Coastal	3.7344	0.9770	3.82	0.0002

(a)

	Estimate	Std. Error	t value	Pr(>|t|)
intercept	2.8234	0.0444	63.54	0.0000
French	-0.4447	0.1482	-3.00	0.0030
Atlas	0.1995	0.1007	1.98	0.0488

(b)

	Estimate	Std. Error	t value	Pr(>|t|)
intercept	14.7805	0.5198	28.44	0.0000
Spanish Coastal	5.0685	1.7406	2.91	0.0040
South Tunisian Coastal	-4.9235	2.0711	-2.38	0.0183

(c)

	Estimate	Std. Error	t value	Pr(>|t|)
intercept	5.1755	0.2108	24.55	0.0000
South Tunisian Coastal	-2.4748	0.7870	-3.14	0.0019
Spanish Coastal	2.6320	0.6618	3.98	0.0001
Algiers	3.1375	0.8330	3.77	0.0002

(d)

	Estimate	Std. Error	t value	Pr(>|t|)
intercept	19.7448	0.6824	28.93	0.0000
Spanish Coastal	7.9483	2.1422	3.71	0.0003
South Tunisian Coastal	-7.1137	2.5473	-2.79	0.0057
Algiers	5.3812	2.6964	2.00	0.0472

(e)

Supplementary Table 6

Gene ID	Annotation	Biological process
Medtr1g045490	calcium-binding EF hand protein	RNA splicing and endonucleolytic cleavage and ligation. Associated to Golgi apparatus and plasma membrane
Medtr2g009110	splicing factor 3B subunit 1	mRNA processing
Medtr3g460780	fasciclin-like arabinogalactan protein	Fasciclin domain-containing proteins are involved in cell adhesion. They may be important during plant shoot development and contribute to plant stem strength, and in response to abiotic stress.
Medtr3g027940	DNA-damage-repair/toleration DRT100-like protein	UV protection and response to UV.
Medtr4g078220	callose synthase-like protein	cell wall. Associated to leaf morphogenesis and to defense response via the salicylic acid mediated signaling pathway
Medtr4g091580	polyubiquitin 3	cellular protein modification process and protein targeting to vacuole. response to UV-B
Medtr5g037410	tyrosine kinase family	protein PTKs are critical components of cellular signaling pathways leading to cell growth and differentiation in animals.
Medtr5g076220	long-chain acyl-CoA synthetase	fatty acid biosynthetic process, mainly long-chain fatty acid metabolic process
Medtr6g033580	sucrose proton symporter 2	AtSUC2 is necessary for efficient transport of sucrose from source (leaves) to sink tissues.
Medtr6g034870	extensin-like region protein	cell wall
Medtr6g034920	extensin-like region protein	cell wall
Medtr6g047750	GRAS family transcription factor	DELLA protein are regulators of gibberellic acid, a plant hormone stimulating plant growth and development.
Medtr6g011890	light-harvesting complex I chlorophyll A/B-binding protein	photosynthesis
Medtr7g060720	PPR containing plant-like protein, putative	Pentatricopeptide repeat (PPR) proteins are a huge family of proteins involved in controlling gene expression in mitochondria and chloroplasts.
Medtr7g023740	polygalacturonase inhibitor	Associated to plant-type cell wall. Involved also in defense response via the abscisic acid and jasmonic acid mediated signaling pathway.

Supplementary Table 7

Gene name	chrom.	position	Pop.1 dN/dS	Pop.2 dN/dS	Pop.3 dN/dS	Pop.4 dN/dS	Pop.5 dN/dS	Pop.6 dN/dS	Pop.7 dN/dS	Pop.8 dN/dS	dN/dS max.	C.V.
Medtr2g091025	chr2	39142715	4.33	3.67	7.00	11.00	7.00	4.33	4.00	4.33	11.00	44.0
Medtr3g028210	chr3	8944365	3.00	6.00	6.00	6.00	6.00	2.00	2.00	3.00	6.00	44.9
Medtr4g065007	chr4	24342256	1.75	1.75	6.00	6.00	6.00	1.50	6.00	2.33	6.00	57.2
Medtr4g080990	chr4	31294716	6.00	2.33	2.67	2.67	5.00	2.67	2.67	7.00	7.00	47.5
Medtr5g026500	chr5	10886269	7.00	–	–	3.00	–	–	2.33	3.50	7.00	52.6
Medtr5g058000	chr5	23939885	10.00	2.50	5.00	5.00	5.00	5.00	5.00	2.50	10.00	46.3
Medtr5g090170	chr5	39278448	2.60	2.60	2.60	2.60	2.60	2.60	2.60	9.00	9.00	66.5
Medtr7g029280	chr7	10342607	–	3.00	9.00	4.50	–	3.00	3.00	3.00	9.00	56.5
Medtr8g043650	chr8	16776123	3.50	2.67	3.50	2.67	7.00	2.67	2.67	2.67	7.00	43.8
Medtr8g013910	chr8	4296399	8.00	4.00	2.00	2.00	2.00	2.00	2.00	2.00	8.00	71.3

Supplementary Table 8

Gene ID	Annotation	Biological process
Medtr2g091025	frigida-LIKE protein	FRIGIDA confers a vernalization requirement in *Arabidopsis thaliana* . Independent loss-of-function alleles that result in a rapid-cycling habit in different accessions.
Medtr3g028210	anthocyanin 5-aromatic acyltransferase anthocyan.	Biological process unknown.
Medtr4g065007	2-oxoglutarate/malate translocator	The 2-oxoglutarate/malate translocator gene has an important role during seed storage in pea (*Pisum sativum*).
Medtr4g080990	carboxy-terminal domain cyclin	DNA endoreduplication, regulation of cell cycle.
Medtr5g026500	3-hydroxy-3-methylglutaryl-coenzyme A reductase-like protein	HMGR catalyzes the first step of isoprenoid biosynthesis. In plants, this pathway provides precursors for for diverse functions, including membrane biogenesis, defense, and control of growth and development.
Medtr5g058000	F-box/RNI/FBD-like domain protein, putative	Biological process unknown.
Medtr5g090170	PPR containing plant-like protein	Pentatricopeptide repeat (PPR) proteins are involved in controlling gene expression in mitochondria and chloroplasts.
Medtr7g029280	Transmembrane protein, putative	Transcription factor of the CCHC(Zn) class.
Medtr8g043650	MADS-box transcription factor family protein	Transcription factor activity. Biological process unknown.
Medtr8g013910	Elongation factor 1-alpha	Translation and nuclear export of proteins.

Supplementary Table 9

	nodules below 5 cm	nodules above 5 cm	total number of nodules	plant height	number of leaves
nodules below 5 cm	1.00	0.50	0.96	0.11	-0.01
nodules above 5 cm	0.50	1.00	0.72	-0.09	0.13
total number of nodules	0.96	0.72	1.00	0.06	0.03
plant height	0.11	-0.09	0.06	1.00	0.10
number of leaves	-0.01	0.13	0.03	0.10	1.00

Supplementary Table 10

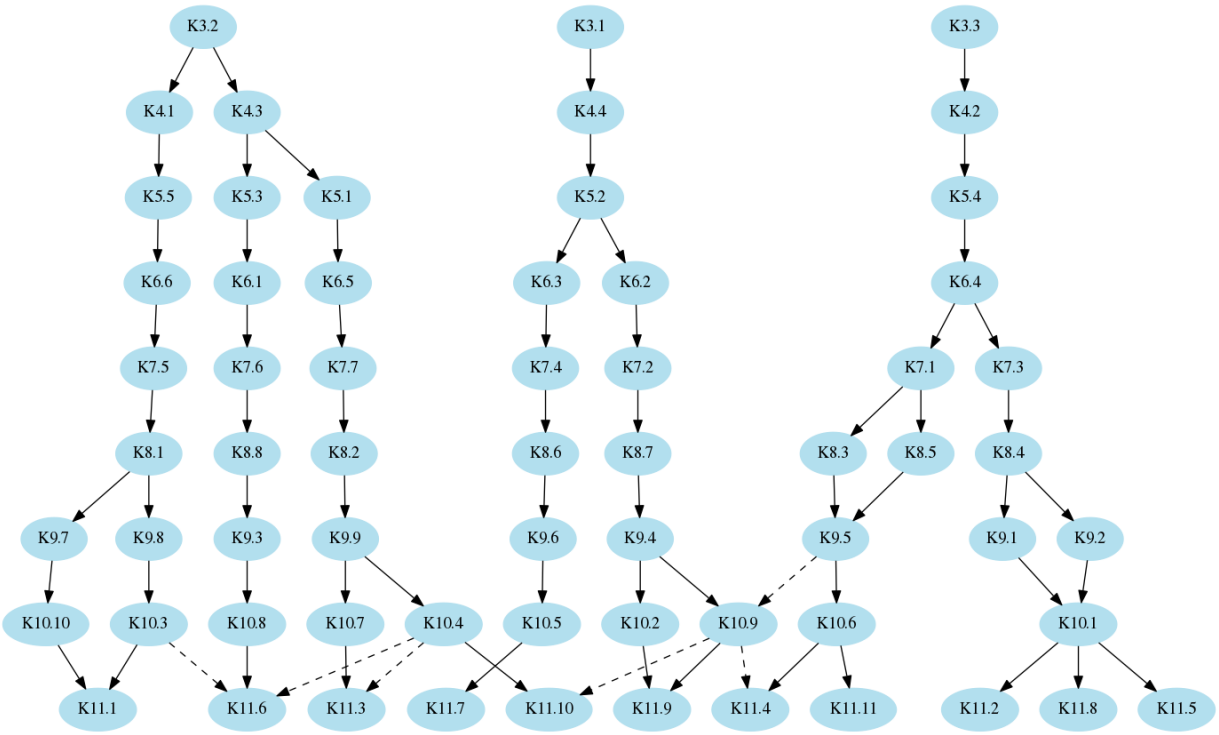

Supplementary Figure 1

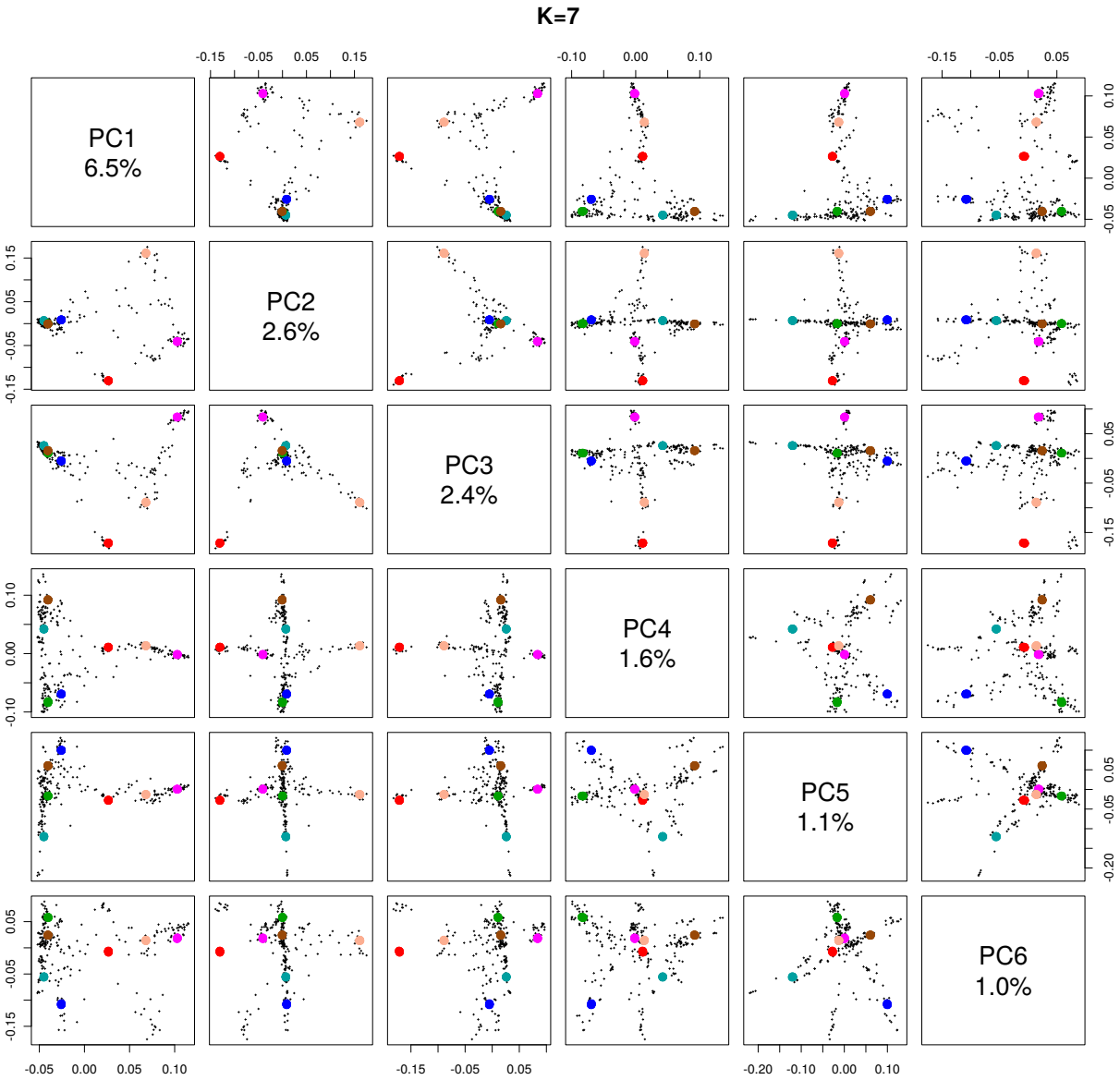

Supplementary Figure 2

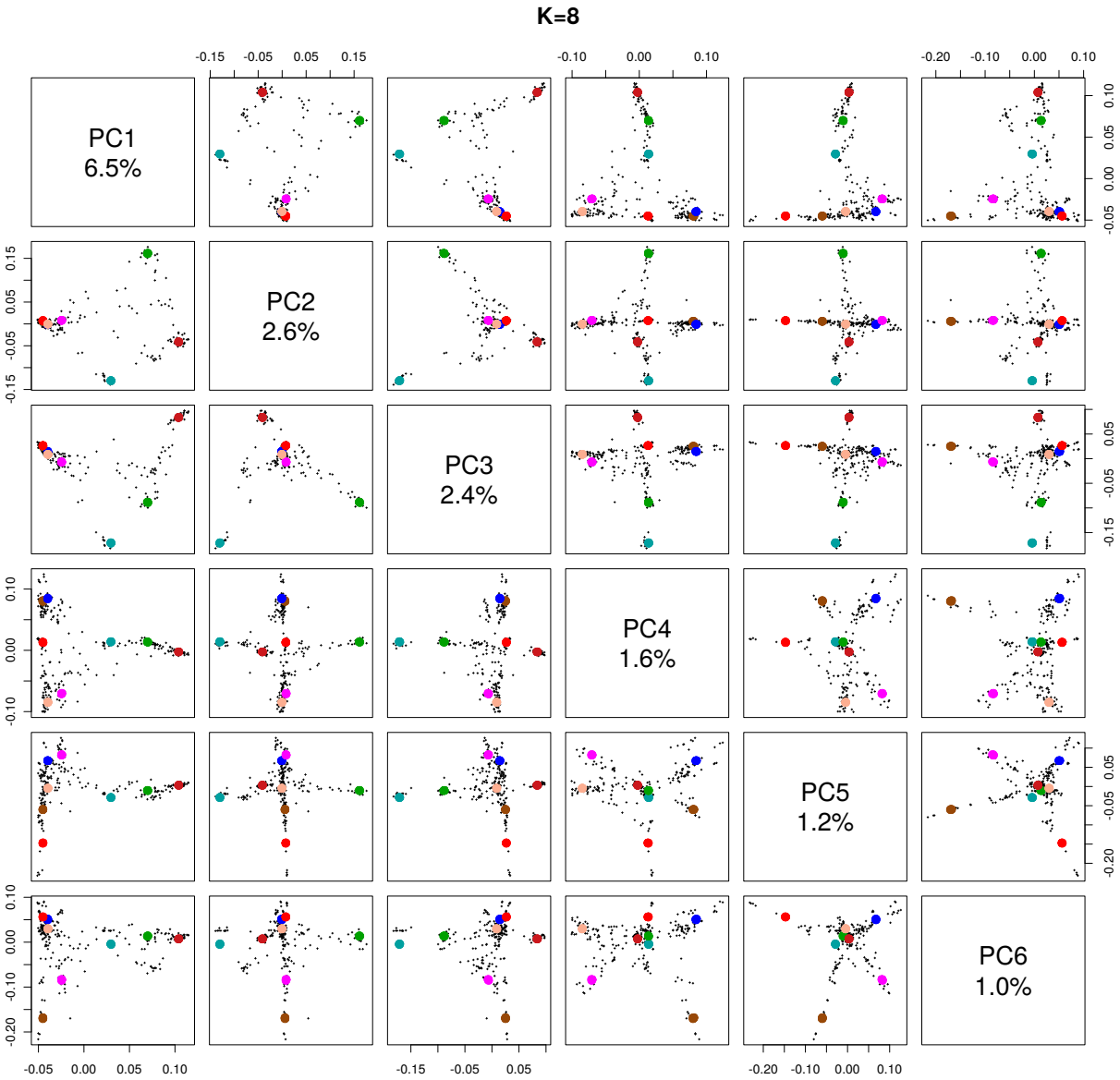

Supplementary Figure 3

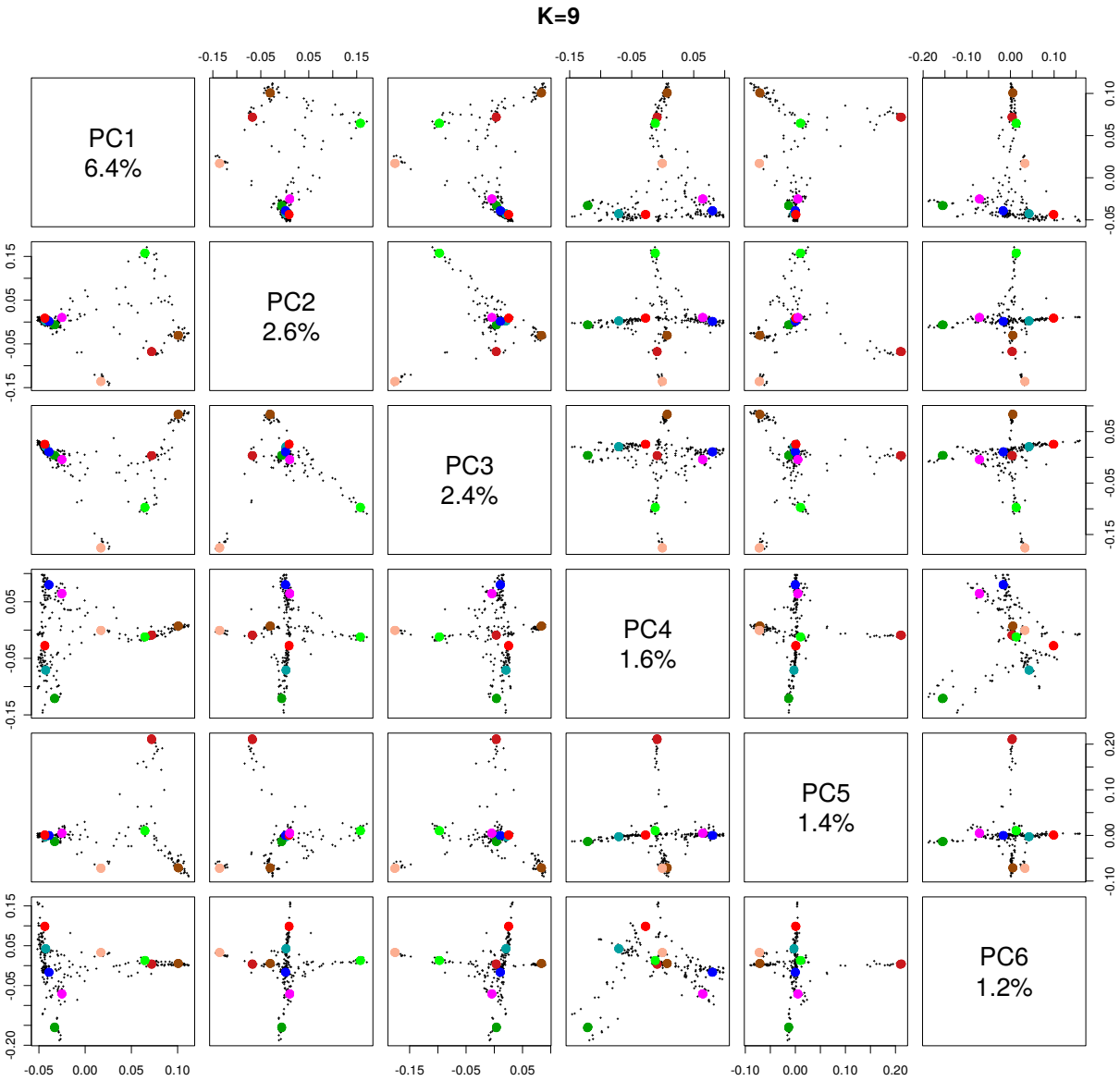

Supplementary Figure 4

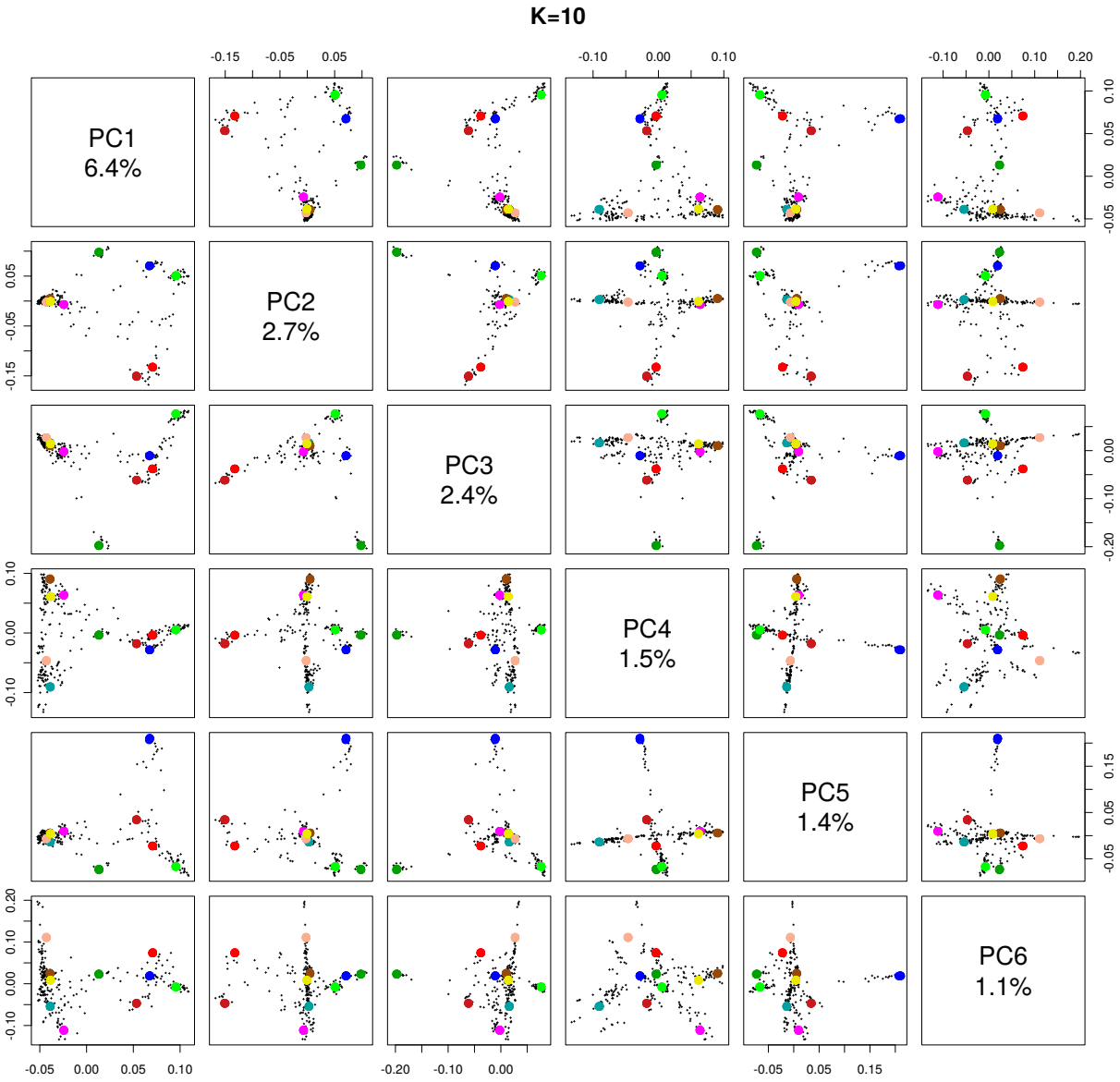

Supplementary Figure 5

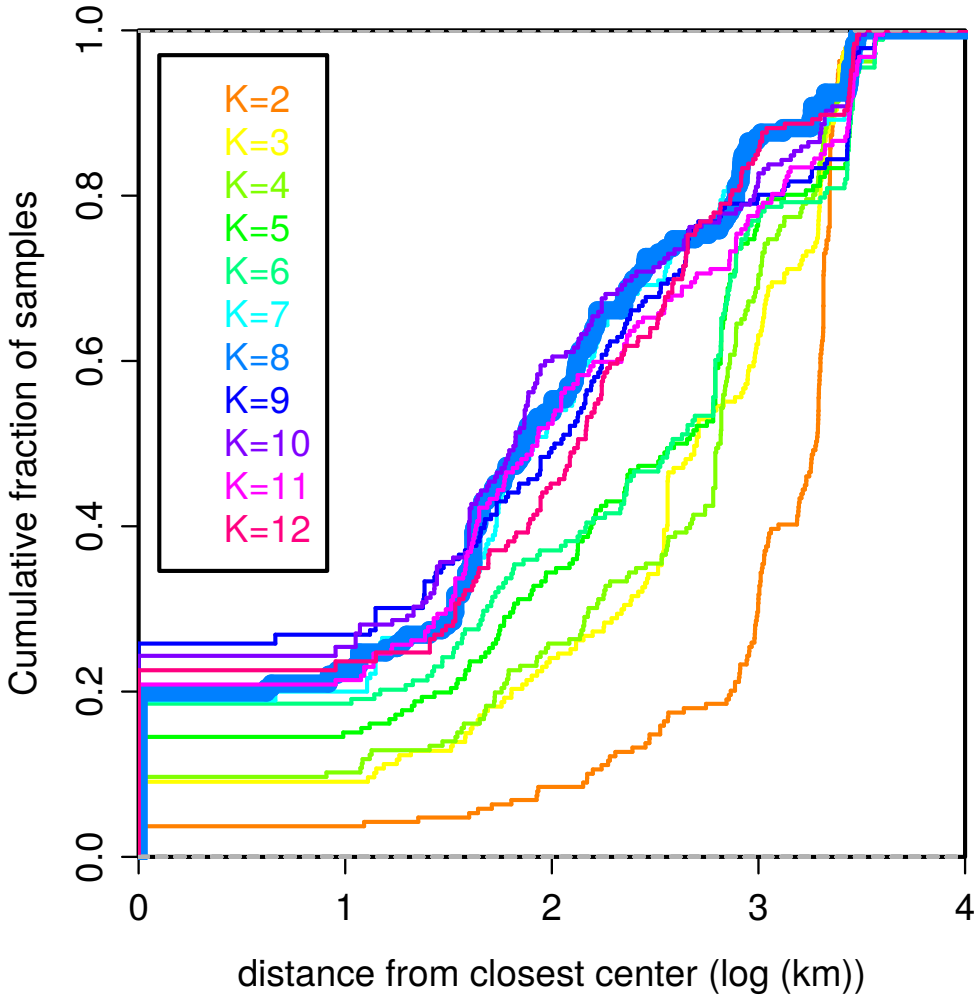

Supplementary Figure 6

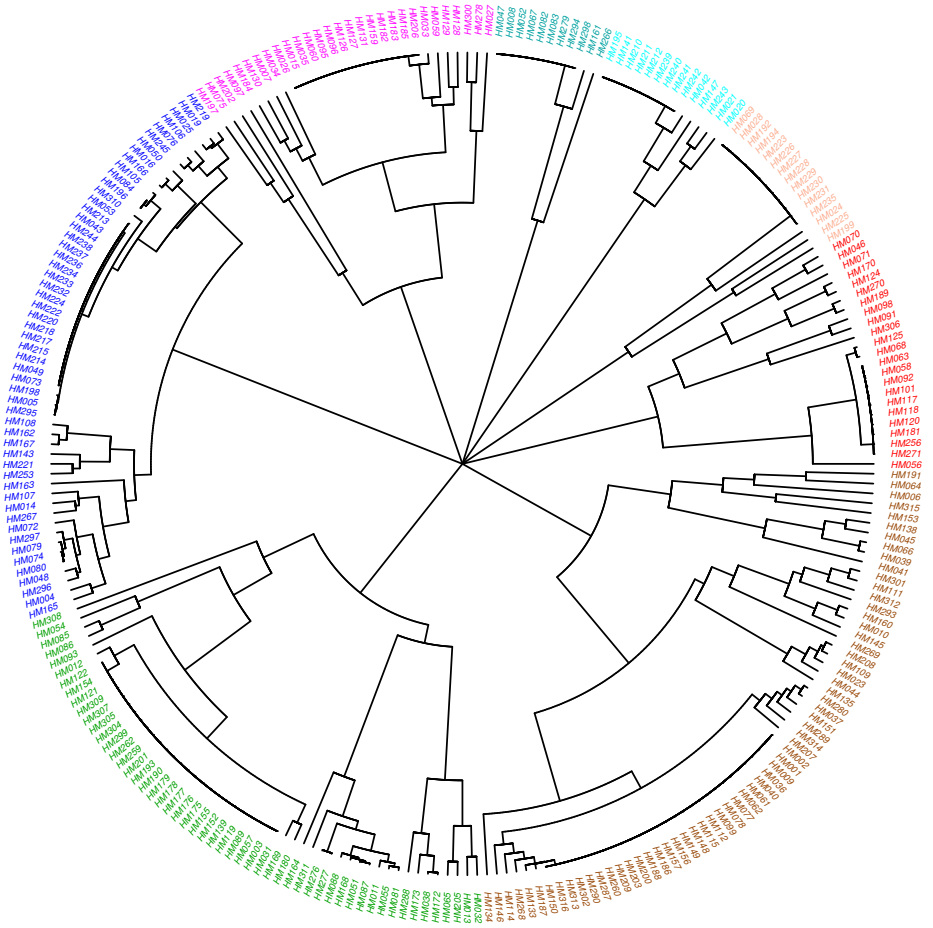

Supplementary Figure 7

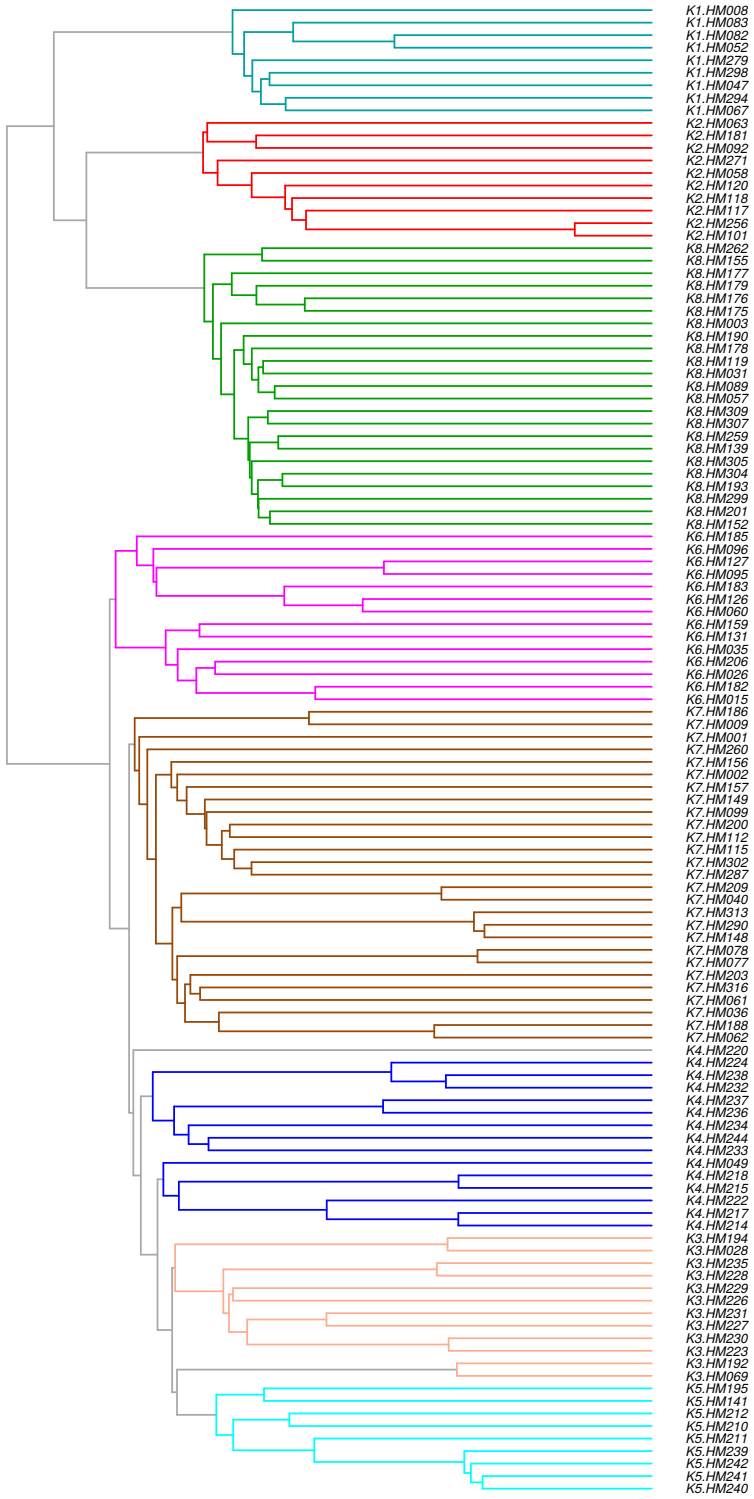

Supplementary Figure 8

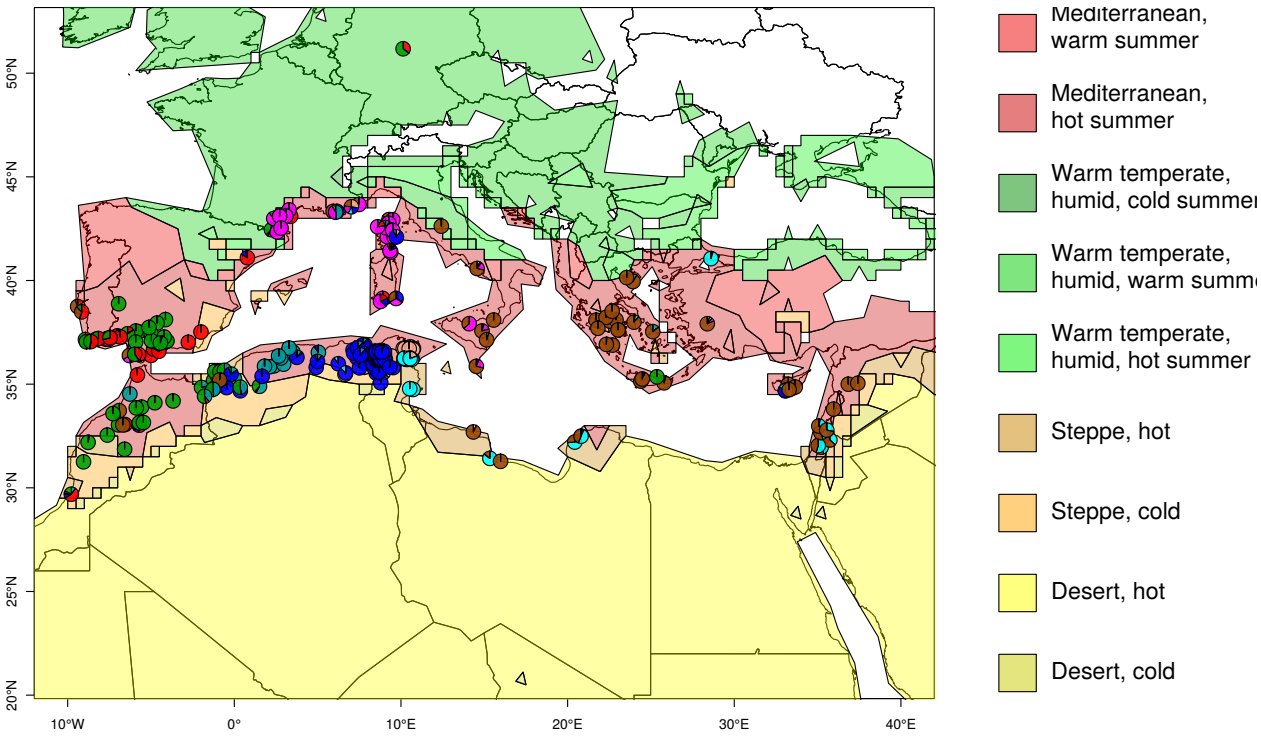

Supplementary Figure 9

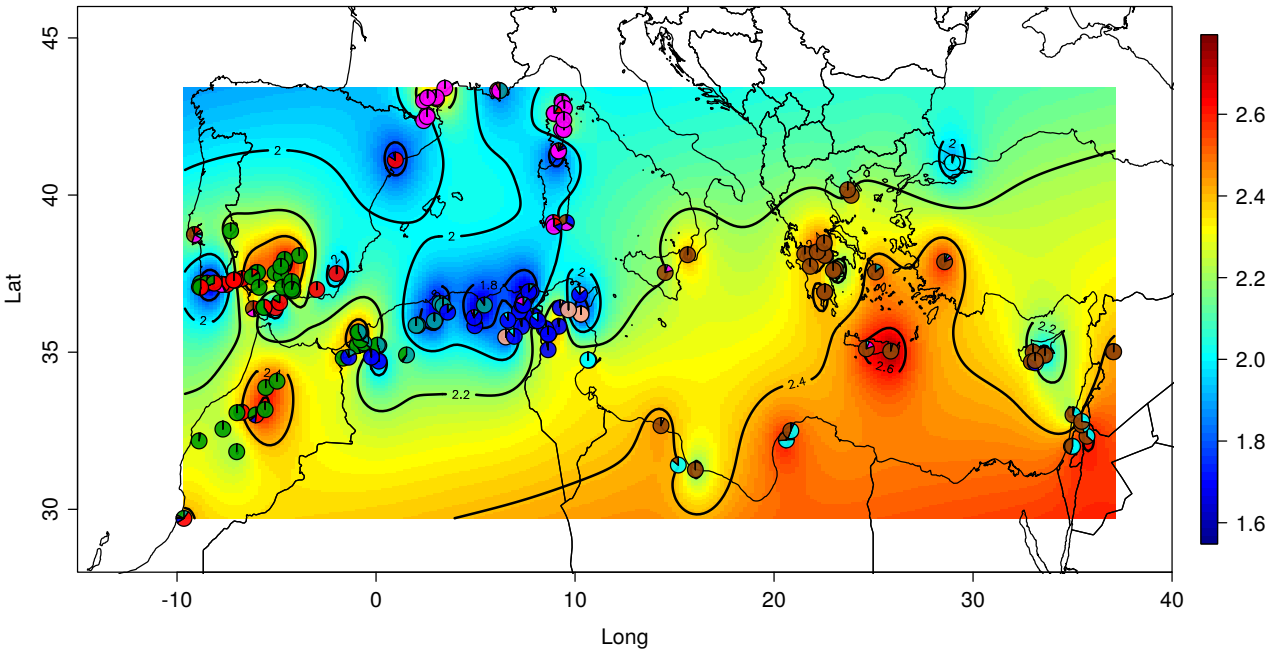

Supplementary Figure 10

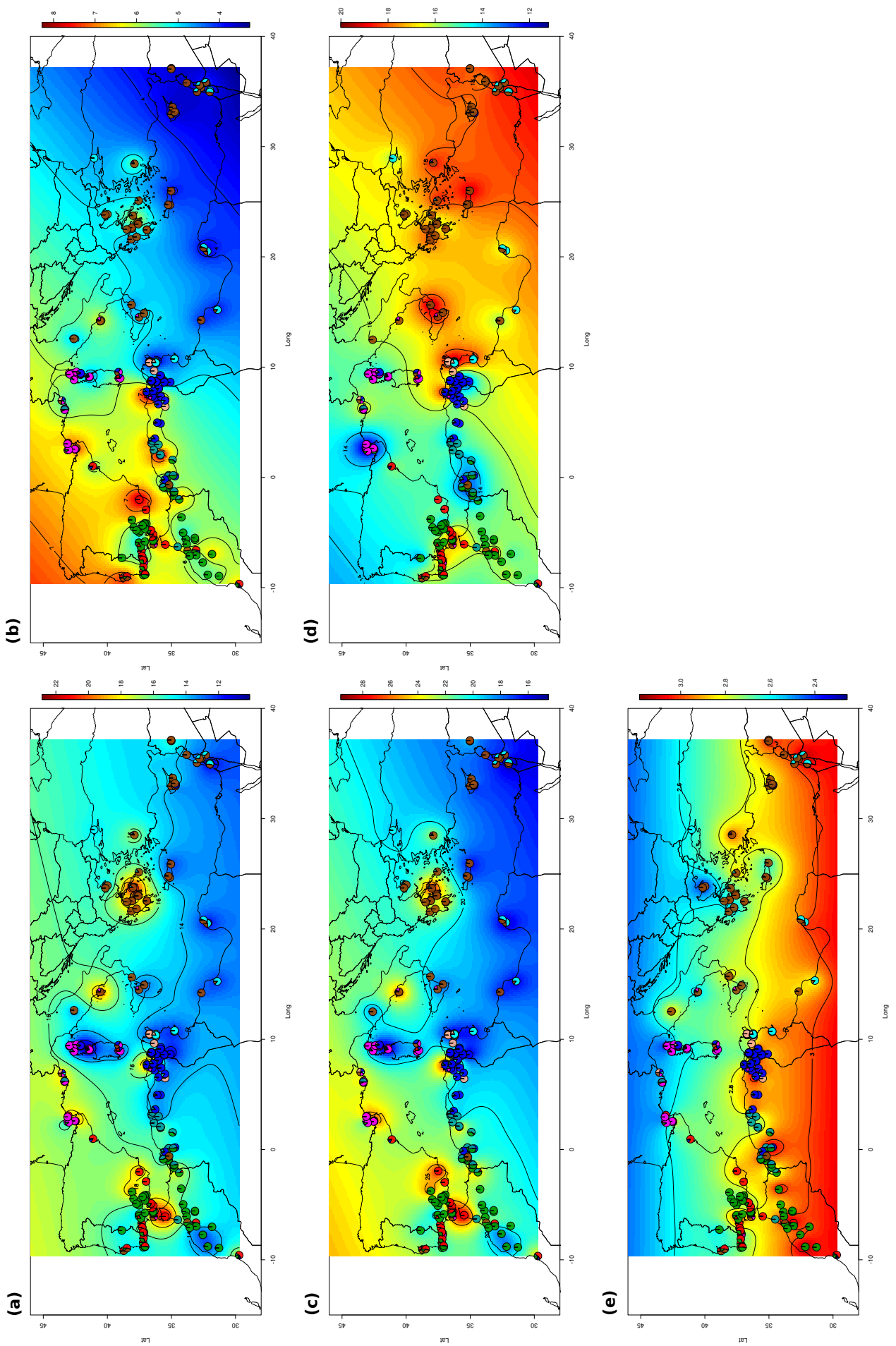

Supplementary Figure 11

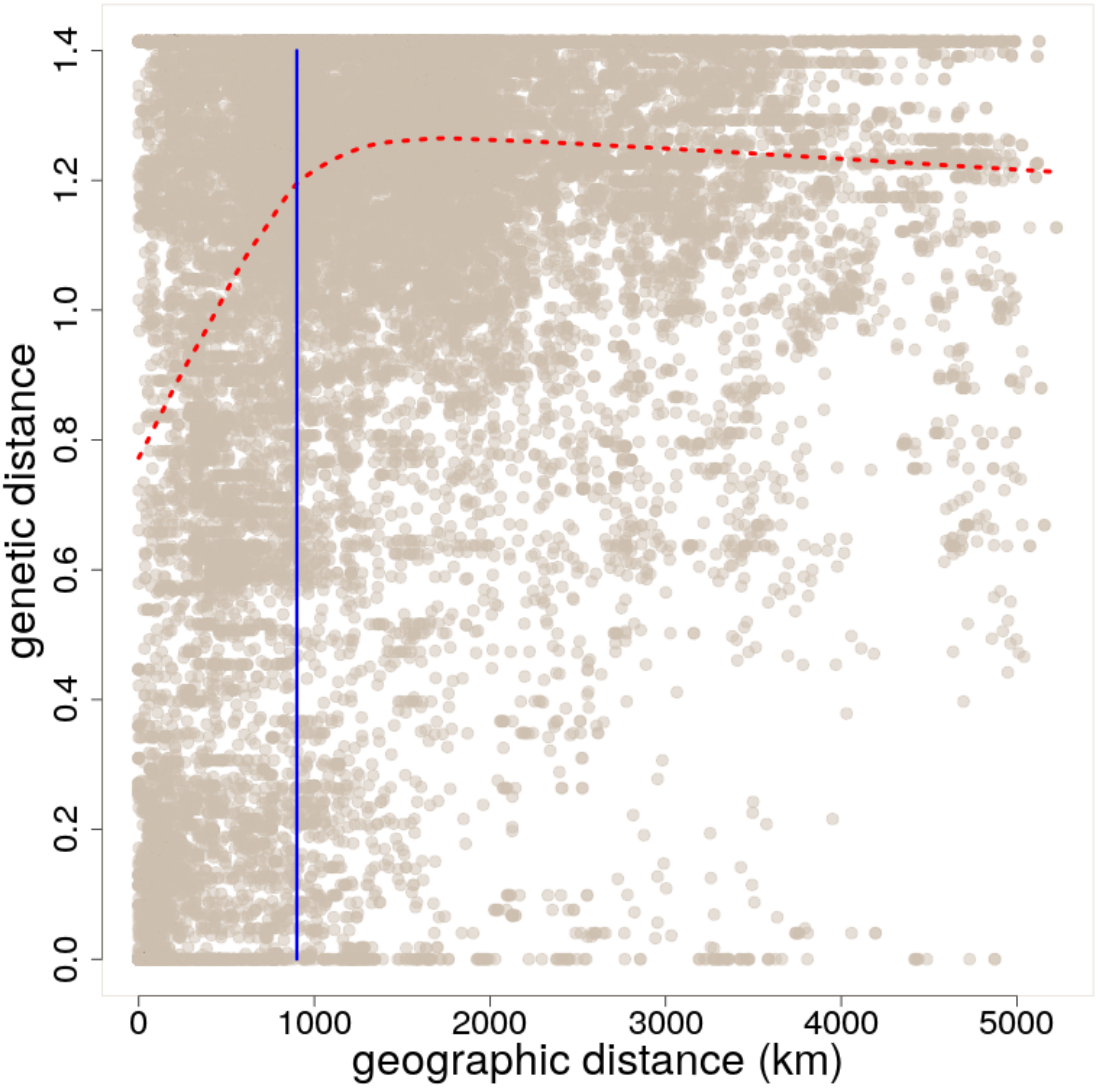

Supplementary Figure 12

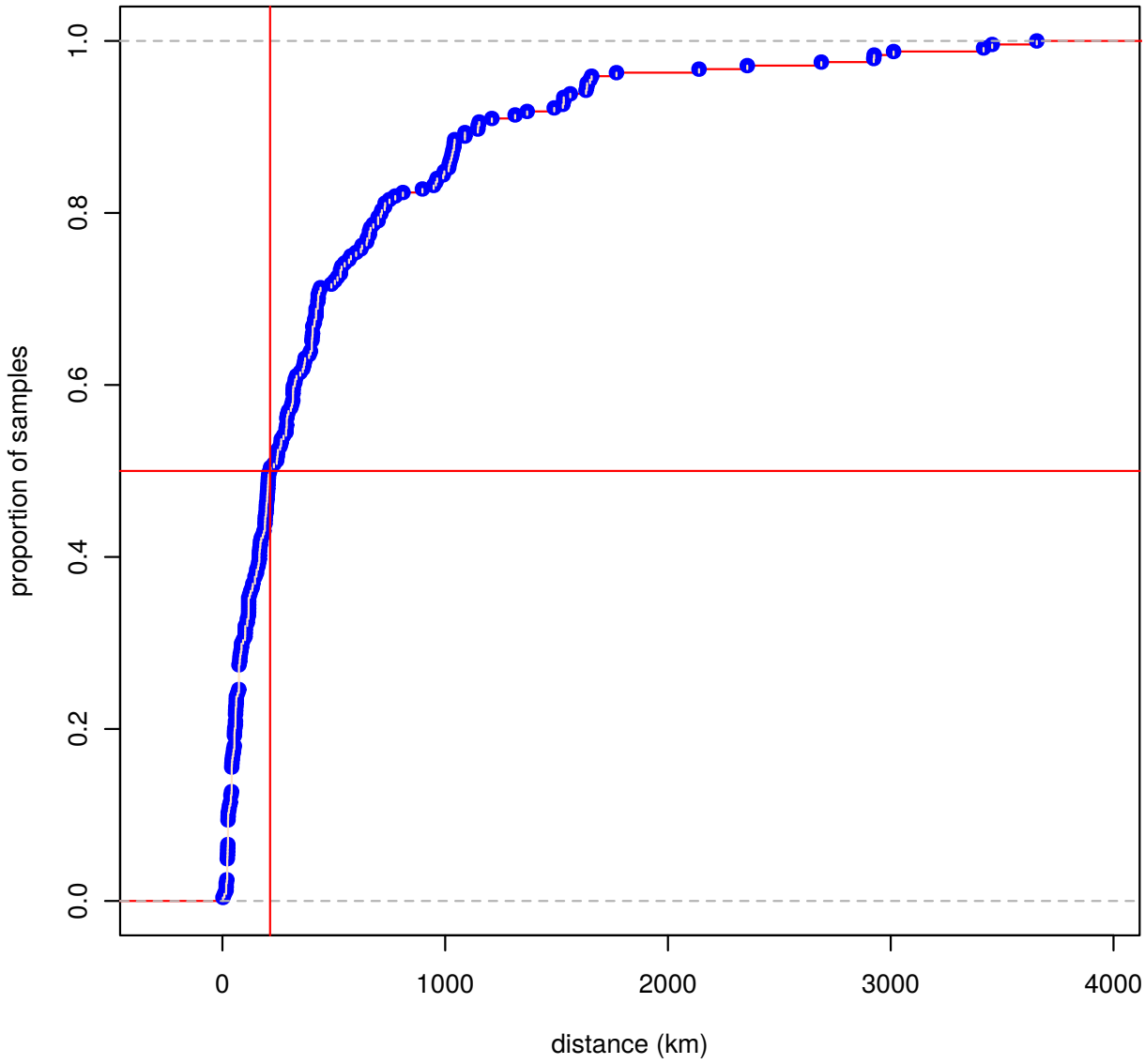

Supplementary Figure 13